



# Synthesis and characterization of three-dimensional carbon foams–LiFePO<sub>4</sub> composites

Lucangelo Dimesso\*, Christina Spanheimer, Susanne Jacke, Wolfram Jaegermann

Darmstadt University of Technology, Materials Science Department, Surface Investigation Division, Petersenstrasse 32, D-64287 Darmstadt, Germany

## ARTICLE INFO

### Article history:

Received 12 August 2010  
Received in revised form 2 November 2010  
Accepted 3 November 2010  
Available online 11 November 2010

### Keywords:

Lithium ion batteries  
Olivine  
Composites  
Carbon foam

## ABSTRACT

The characterization of three-dimensional (3D) carbon foams coated with olivine structured lithium iron phosphate is reported for the first time. The LiFePO<sub>4</sub> as cathode material for lithium ion batteries was prepared by a Pechini-assisted reversed polyol process. The coating has been successfully performed on commercially available 3D-carbon foams by soaking in aqueous solution containing lithium, iron salts and phosphates at 70 °C for 2–4 h. After drying-out, the composites were annealed at different temperatures in the range 600–700 °C for 15–20 min under nitrogen. The formation of the olivine-like structured LiFePO<sub>4</sub> was confirmed by X-ray diffraction analysis performed on the powder prepared under similar conditions. The surface investigation of the prepared composites showed the formation of a homogeneous coating by LiFePO<sub>4</sub> on the foams. The cyclic voltammetry curves of the composites show an enhancement of electrode reaction reversibility by decreasing the annealing temperature. The electrochemical measurements on the composites showed good performances delivering a discharge specific capacity of 85 mAh g<sup>-1</sup> at a discharging rate of C/25 at room temperature.

© 2010 Elsevier B.V. All rights reserved.

## 1. Introduction

Among the new cathode materials that can replace the presently used transition metal oxide based materials in lithium batteries, the transition metals containing phosphates (LiMPO<sub>4</sub>, with M = Fe, Co, Ni, Mn) have gained considerable interest. Since the discovery by Padhi [1], lithium iron phosphate (LiFePO<sub>4</sub>) is a promising cathode material due to its good thermal stability, the relatively low costs for synthesis and low environmental impact [2]. The LiFePO<sub>4</sub> operates at a flat voltage of 3.4 V vs. Li<sup>+</sup>/Li, yields a theoretical specific capacity of 170 mAh g<sup>-1</sup>, and a theoretical gravimetric energy density comparable to that of LiCoO<sub>2</sub>. However one of the main drawbacks of olivine LiFePO<sub>4</sub> for the commercial application is its low electronic conductivity and low lithium-ion diffusivity across the LiFePO<sub>4</sub>/FePO<sub>4</sub> interface [3] during the charge/discharge processes. Thus, in order to enhance the overall kinetics many efforts have been performed to overcome the problems of poor conductivities of electron and lithium ion by several strategies such as metal-doping, synthesizing fine particles [4,5] and carbon-coating on the LiFePO<sub>4</sub> surface [6–9]. In fact, the carbon coating increases the amount of electrode/electrolyte interface enhancing the charge transport of the lithium ions and consequently improving the electrochemical properties of the lithium ion batteries.

A new approach to enhance the effects of the carbon content has been reported by Bhuvanewari et al. [10], based on the addition of functionalized carbon nanofibers (two-dimensional system, hereafter CNFs) during the sol–gel synthesis of LiFePO<sub>4</sub>. The authors found out that an oxidative wet functionalization of the CNFs by concentrated nitric acid gives better adhesion of LiFePO<sub>4</sub> particles on their surface. Moreover, the additional surface of the carbon nanofibers offered an efficient method for increasing the interfacial area and decreasing the lithium ion diffusion distance, allowing for fast charge transport and improved power capability (specific capacity of 120 mAh g<sup>-1</sup> at a charge rate of 0.1 C) compared to acetylene black added LiFePO<sub>4</sub> even though the coating was not homogeneous.

Improved battery performance can be achieved by reconfiguring the electrode materials currently employed in 2D batteries into 3D architectures. Improvements in energy per unit area and high-rate discharge capabilities are two of the benefits that may be realized for these 3D cells. Among the different 3D architectures example for charge-insertion batteries [11], the aperiodic “sponge” architecture can be effective. Efficient access of the electrolyte into the electrode pores is essential to harness the advantages that porous electrode materials might offer. Micropores, with diameters less than 2 nm, can produce very high surface areas. However, they are easily blocked, may not allow efficient access of the electrolyte throughout the electrode, and therefore may not be ideal for electrode materials. Electrode materials with slightly larger pores, mesopores in the range 2–50 nm, also offer high surface areas while potentially avoiding the permanent trapping of lithium ions that

\* Corresponding author. Tel.: +49 0 6151 16 69667; fax: +49 0 6151 16 6308.  
E-mail address: [ldimesso@surface.tu-darmstadt.de](mailto:ldimesso@surface.tu-darmstadt.de) (L. Dimesso).

is possible with micropores. Recently Doherty [12] reported the preparation of  $\text{LiFePO}_4/\text{Carbon}$  composite monolith by nanocasting technique. The authors succeeded to prepare composites with capacity of  $140 \text{ mAh g}^{-1}$  attained at a discharge rate of 0.1 C and  $100 \text{ mAh g}^{-1}$  at 5 C. However, this process, which includes the preparation of meso/macroporous silica monolith and a chemical etch of the monolith after carbonization, is time consuming.

A valid alternative is the use of commercially available carbon foams. The role of the carbon foams is: (i) they ensure good inter-particle conductivity and (ii) the continuous macroporous network allows an efficient transport route for the solvated ions to get to the mesopores and hence may offer superior battery performances. One more important feature of the carbon is to slow or prevent detrimental corrosion processes in the batteries [13,14 and references herein]. The use of carbon foams has several advantages: (i) they have low specific resistance ( $400\text{--}2500 \mu\Omega\text{m}$ ); (ii) they allow easier assembly of the positive and negative collectors that operate together in the battery; (iii) the porosity of the carbon foam allows a greater infiltration of the electrolyte into the battery leading to a better electrical contact; (iv) many configurations are possible depending on the particular applications. Additionally, carbon foam is lightweight due to the presence of a network of pores and may include a total porosity value of at least 60%. In fact, commercially available carbon foams may have an open porosity of at least 90% resulting in a density of less than about  $0.6 \text{ g cm}^{-3}$ .

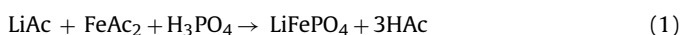
Similar advantages can be used for manufacturing lithium ion batteries. Lithium ion batteries provide several advantages over known lead batteries, such as small self-discharge characteristic and environmental safety. But the greatest advantage of lithium ion batteries over the known battery for vehicle application is the attractive energy-density-to-weight ratio. Although a lot of work over  $\text{LiFePO}_4/\text{C}$  composites has been reported in literature, the authors have found a few references [12,15,16], dealing with the characterization of carbon foams– $\text{LiFePO}_4$  composites.

The properties of the composites are greatly affected by several parameters such as particle size, morphology, purity and chemical composition. Recently Dimesso [17] has reported the preparation of composites of three-dimensional amorphous carbon coated with  $\text{LiFePO}_4$  by a Pechini-assisted reversed polyol method. The process consists of a very simple citrate gel method by using simple water soluble inorganic salts, the process utilizes the ability of certain  $\alpha$ -hydroxycarboxylic acids, such as citric acid, lactic and glycolic acids to form polybasic acid chelates with transition metals. The chelates can undergo polyesterification when heated with a polyhydroxy-alcohol (i.d. ethylene glycol in [18]). Calcination of the resin removes the organic constituents leaving the desired ceramic composition as the residue. This process can avoid complex steps in the preparation of materials, resulting in less time consumption compared to other techniques [19].

Following the previously results [17] we report, for the first time, the synthesis of 3D carbon foams– $\text{LiFePO}_4$  composites (hereafter CF–LFP), prepared by the Pechini-assisted reversed polyol method, using water as solvent. For comparison, pure  $\text{LiFePO}_4$  (hereafter LFP) has been also prepared under similar conditions. The composites have been characterized by XRD, SEM and electrochemical analyses. The electrochemical performances have been discussed in relation to the structural and to the morphological investigation.

## 2. Experimental

The preparation of the pure  $\text{LiFePO}_4$  cathode material by the polyol method is based on the acid–base reaction of the metal acetates with ammonium hydrogen phosphate in a polyol according to reaction (1)



where HAc indicates acetic acid. A detailed description of the Pechini-assisted reverse polyol method has been previously reported [16]. The  $\text{LiFePO}_4$  samples are prepared by dissolving in water  $\text{Li}(\text{CH}_3\text{COO})\cdot 2\text{H}_2\text{O}$  (lithium acetate),  $\text{Fe}(\text{SO}_4)_2\cdot 7\text{H}_2\text{O}$  (iron(II) sulfate) as precursors (molar ratio 1:1) with citric acid ( $2 \times \text{mol} [\text{Fe}]$ ), then adding the polyol (e.g.: di-ethylene glycol) till the water weight percentage reached the desired value. Finally, phosphoric acid in equimolar ratio with Li and Fe ions was added.

In order to find the most proper conditions of synthesis, several experiments have been performed with different starting concentrations of the reagents (ranging between 0.05 M and 0.2 M), with different water contents at different temperatures. In this work, water was added to reach the final starting concentration. Pure water, due to the rheological properties, favored the infiltration of the ions containing solution into the porous architecture of the foams. The starting solution, with a concentration of the precursors of 0.1 M, was heated up to  $80\text{--}90^\circ\text{C}$  and kept at that temperature for 2–4 h. After cooling down the solution, the product was separated by filtration. Then the precipitate was dried out by heating at  $130^\circ\text{C}$  for 24 h in vacuum. In order to obtain the olivine structured  $\text{LiFePO}_4$  phase, the powder was annealed at different temperatures for 5 h in agreement with the thermal data previously reported.

The commercial foams (GRAFOAM<sup>®</sup> carbon foams, a registered trade name from GRAFTECH International Ltd. [20]) have been cut as disks having 5 mm diameter and 1–2 mm thickness. The composites were prepared by soaking the commercial foams in the starting aqueous solution at  $70^\circ\text{C}$  for 2 h. After soaking, the foams were rinsed slightly with water and dried out by heating at  $130^\circ\text{C}$  for 24 h in vacuum. In order to obtain the olivine structured  $\text{LiFePO}_4$  phase, the powder was annealed at different temperatures ranging from  $600^\circ\text{C}$  to  $700^\circ\text{C}$  for 15 min.

The structural analysis of the samples was performed by X-ray powder diffraction using a D8 Bruker powder diffractometer (Cu  $\text{K}\alpha_1 + \text{Cu} \text{K}\alpha_2$  radiation) with a theta/2 theta Bragg–Brentano configuration. The diffractometer is equipped with an energy dispersion detector Si(Li) to minimize the fluorescence effects. A scanning electron microscope Philips XL 30 FEG was used to investigate the morphology of the samples. Electrochemical studies (e.g.: cyclic voltammetry, CV) have been carried out with a multichannel potentiostatic–galvanostatic system VPM2 (Princeton Applied Research, USA). For the measurements, Swagelok-type cells were assembled in an argon-filled dry box with water and oxygen less than 5 ppm. For the powder, a typical cathode material was fabricated as follows: 85 wt.% active material, 10 wt.% acetylene carbon black and 5 wt.% PTFE (60 wt.% water dispersion, Aldrich) as binder were intimately mixed in a few milliliters of 2-propanol and treated in ultrasound bath for 20 min at RT. The resulting paste-like material was cut in pellets and dried out at  $95^\circ\text{C}$  for 24 h under vacuum (resulting electrode containing 20–30 mg active compound). To measure the composites, the foam disks were direct assembled into the cell and a few drops of the electrolyte were added. In the cell, Li metal was used as anode, Powerlyte (1 M  $\text{LiPF}_6$  in ethylene-carbonate: di-methyl-carbonate 3:7 (wt/wt), Ube Industries, Ltd., Japan) as electrolyte, Celgard<sup>®</sup>2500 as separator. The aluminum current collector was not used. All electrical measurements were performed at room temperature.

## 3. Results and discussion

### 3.1. Structural analysis

In Fig. 1, a typical XRD-pattern of as-prepared LFP reveals the non-crystalline nature of the powder independently of the starting concentration of the solution. The X-ray diffractogram of the as-prepared LFP sample after annealing at  $600^\circ\text{C}$  for 10 h under

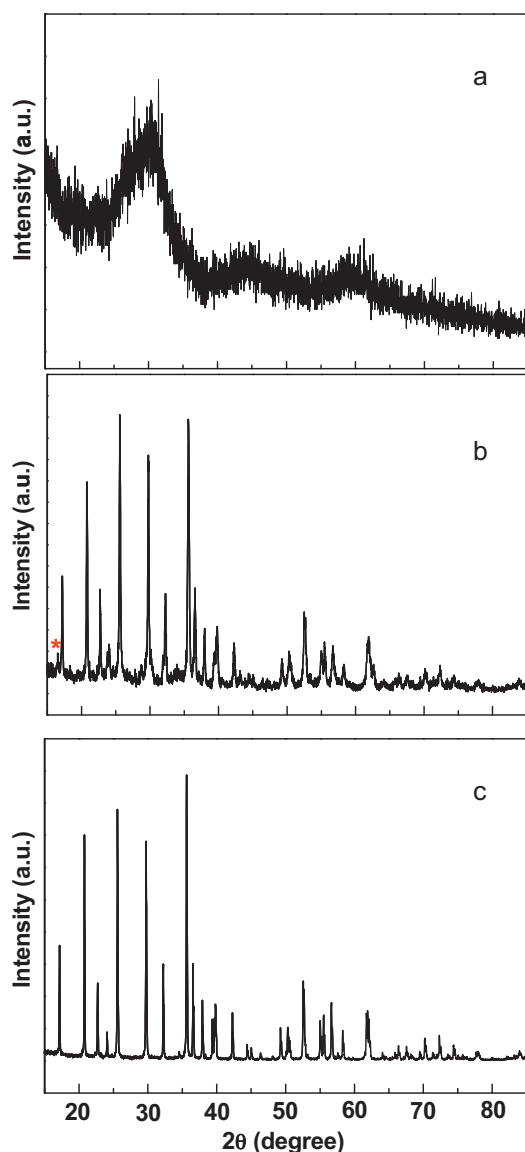


**Fig. 1.** XRD-pattern of  $\text{LiFePO}_4$  samples: (a) as prepared; (b) after annealing at  $600^\circ\text{C}$  for  $t = 10$  h under nitrogen; (c) commercial  $\text{LiFePO}_4$ . Secondary phases are indicated with (\*).

nitrogen atmosphere is shown in Fig. 1b. The XRD patterns of the prepared samples have been compared with the diffractogram of a  $\text{LiFePO}_4$ -containing commercial powder (reported in Fig. 1c). The spectra show the presence of the olivine-like structured  $\text{LiFePO}_4$  as major crystalline phase: however, crystalline reflections attributed to secondary phases have been also detected (indicated with \* in Fig. 1b). Although a deeper investigation on the secondary phases has not been carried out, such peaks could belong, possibly, to Fe-poor phases which usually appear during the decomposition of the LFP phase. The grain size of the samples, estimated by using the Scherrer formula, was 19 nm.

### 3.2. HREM

The important role played by the carbon in the LFP-carbon composites is widely reported in the literature. The micrographs in Fig. 2a–c shows the morphological surface of the used foams. The porous architecture of the foams with hierarchical pore size distribution in micro-, meso-, and macropore ranges can be clearly recognized (Fig. 2a). A closer view shows the presence of numer-

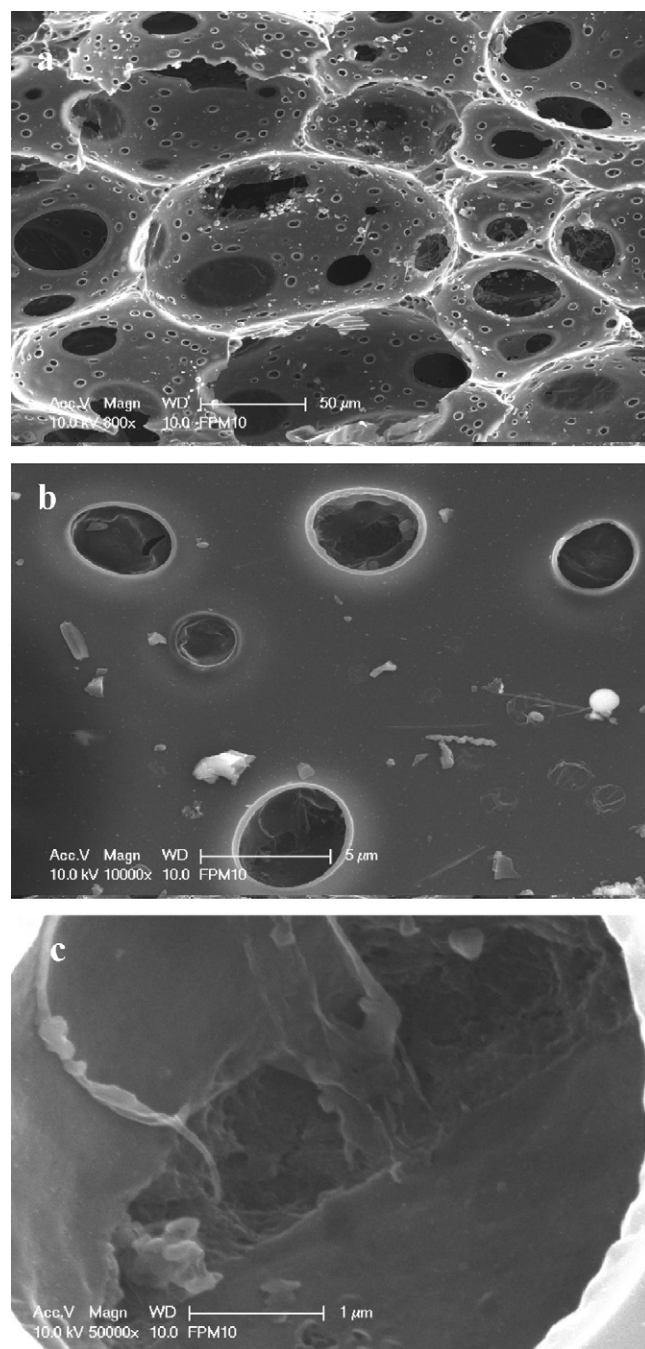


**Fig. 2.** HREM pictures, at different magnifications, of the commercial foam after cutting, rinsing in acetone and drying out.

ous apertures (Fig. 2b), suggesting that the interior pore system is interlaced and the nanoporous architecture is uniform. While the carbon serves as an electron conductor, the pores, when filled with liquid electrolyte, serve as a source of  $\text{Li}^+$  ions. The importance of a porous nanoarchitecture has been previously reported [11]. The authors emphasize that in this “sponge” approach, the electrolyte layer is formed around a random 3D network of electrode material. This design strategy also represents a concentric configuration in that the electrolyte envelops the electrode material while the other electrode material fills the macroporous and mesoporous spaces. Short transport-path characteristics between the insertion electrodes are preserved with this arrangement.

The micrographs of the CF-LFP composites prepared by soaking before and after annealing at  $600^\circ\text{C}$  for 10 min under nitrogen



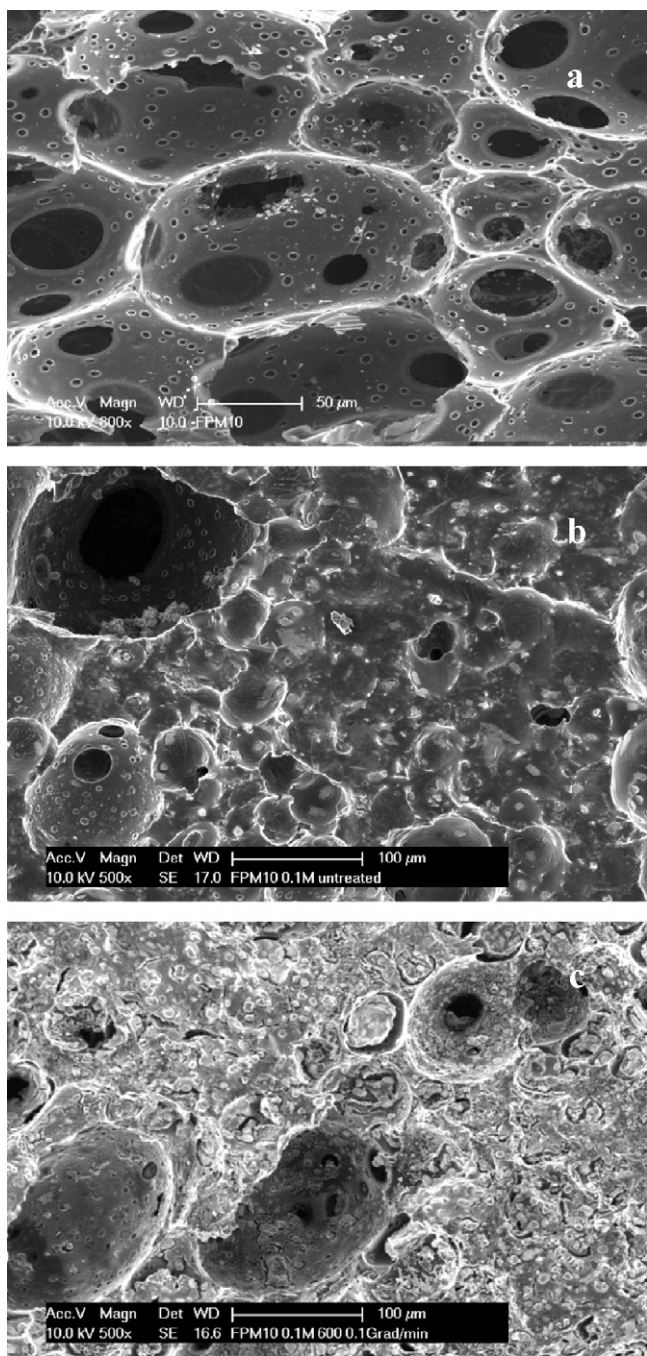


**Fig. 3.** HREM pictures of (a) carbon foam as delivered; (b) carbon foam–LiFePO<sub>4</sub> composites before annealing at  $T = 600\text{ }^{\circ}\text{C}$ ; (c) carbon foam–LiFePO<sub>4</sub> composites after annealing at  $600\text{ }^{\circ}\text{C}$  for 10 min prepared by soaking.

are shown in Fig. 3a–c. The micrograph shows a very homogeneous coating of the foam surface and consequently a more homogeneous morphology. By soaking, the foam surface is covered by a continuous layer of liquid in which the  $\text{Li}^+$ ,  $\text{Fe}^{2+}$  and  $(\text{PO}_4)^{3-}$  ions are uniformly distributed. The slow evaporation of the solvent leads to a “uniform” layer on the foam surface (Fig. 3b). After annealing under nitrogen, the formation of a uniform layer of crystalline LiFePO<sub>4</sub> can be observed (Fig. 3c).

### 3.3. Electrochemical measurements

Electrochemical measurements have been performed both on the “pure” olivine and on the composites prepared by soaking and

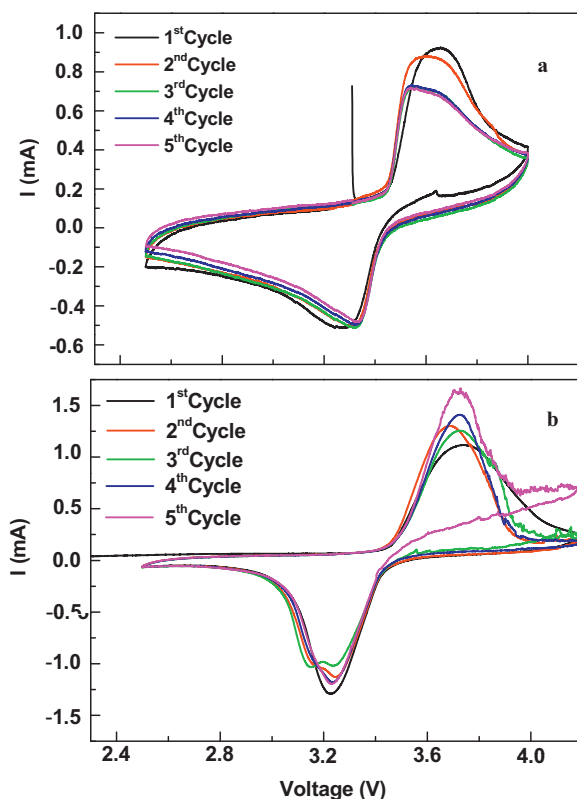


**Fig. 4.** Cyclic voltammograms recorded for LiFePO<sub>4</sub> after annealing under nitrogen at: (a)  $T = 600\text{ }^{\circ}\text{C}$ ; (b)  $T = 650\text{ }^{\circ}\text{C}$  (scan rate  $0.05\text{ mV s}^{-1}$ , in the potential range 2.5–4.0 V vs.  $\text{Li}^+/\text{Li}$ ).

annealed at different temperatures under nitrogen. The elemental analysis (CHNX-analysis) for LiFePO<sub>4</sub> indicates the presence of 18.0 wt.% of amorphous carbon content in the sample. To keep the results consistent, the calculations were performed on the active material only; hence the mass of the carbon was subtracted.

CV curves were recorded for LFP after annealing at different temperatures, using Li metal as counter and reference electrode and are shown in Fig. 4a and b, respectively. The CV curves indicate the potential range in which the lithium deintercalation/intercalation occurs and the phase transitions (if there is any) occur during this process. The deintercalation/intercalation potentials corresponding to the mean peak maxima as in Fig. 4a and b are shown in Table 1. The values clearly indicate that, although the CV profiles are almost reduplicate from the third cycle only, the kinetics of the lithium deintercalation and intercalation is slightly improved in the sample annealed at lower temperature.

The CV curves for the CF–LFP composites are shown in Fig. 5a–c. The corresponding deintercalation/intercalation potentials at the mean peak maxima as in Fig. 5a–c are shown in Table 2. The measurements indicate clearly an improved kinetics of the lithium deintercalation/intercalation processes in the composites annealed

**Table 1**  
Values of the deintercalation/intercalation potentials (peak maxima in Fig. 4a and b) for LiFePO<sub>4</sub> samples after annealing under nitrogen at different temperatures.

Annealing temperature ( $^{\circ}\text{C}$ )	Cycle (nr)	Deintercalation potential (V)	Intercalation potential (V)
600	1	3.65	3.26
	2	3.60	3.30
	3,4,5	3.50	3.30
650	1	3.75	3.23
	2	3.68	3.25
	3,4,5	3.72	3.23

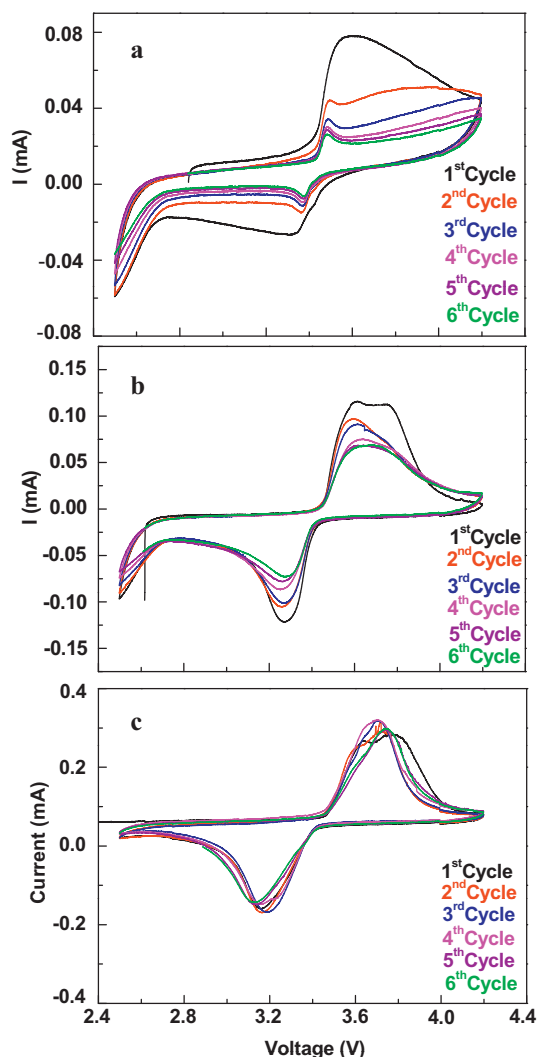


**Fig. 5.** Cyclic voltammograms recorded for the carbon foam–LiFePO<sub>4</sub> composites after annealing at: (a)  $T = 600\text{ }^{\circ}\text{C}$ ; (b)  $T = 650\text{ }^{\circ}\text{C}$ ; (c)  $T = 700\text{ }^{\circ}\text{C}$ , respectively (scan rate  $0.05\text{ mV s}^{-1}$ , in the potential range 2.5–4.2 V vs. Li<sup>+</sup>/Li).

at lower temperature ( $600\text{ }^{\circ}\text{C}$ ). The polarization in the first cycle is obvious and peak voltage separation is  $0.30\text{ V}$  in the first cycle, while it is only  $0.10\text{ V}$  from the second cycle (Fig. 5b). This is probably due to the fact that lithium diffusion and electrochemical kinetics reach an optimal state after the initial cycle. In the composite cathode, well-developed CV loop confirms that the kinetics of lithium intercalation and deintercalation is markedly improved compared to pure LiFePO<sub>4</sub>. The very small difference between oxidation and reduction potentials could indicate a very small polarization occurring in the composites. At higher annealing temperatures, the higher peak voltage separation indicates clearly that electrochem-

**Table 2**

Values of the deintercalation/intercalation potentials (peak maxima in Fig. 5a–c) for the carbon foam–LiFePO<sub>4</sub> composites after annealing under nitrogen at different temperatures.

Annealing temperature ( $^{\circ}\text{C}$ )	Cycle (nr)	Deintercalation potential (V)	Intercalation potential (V)
600	1	3.60	3.30
	2,3,4,5,6	3.50	3.40
650	1	3.70	3.30
	2,3,4,5,6	3.60	3.20
700	1	3.80	3.16
	2,3,4,5,6	3.60	3.10

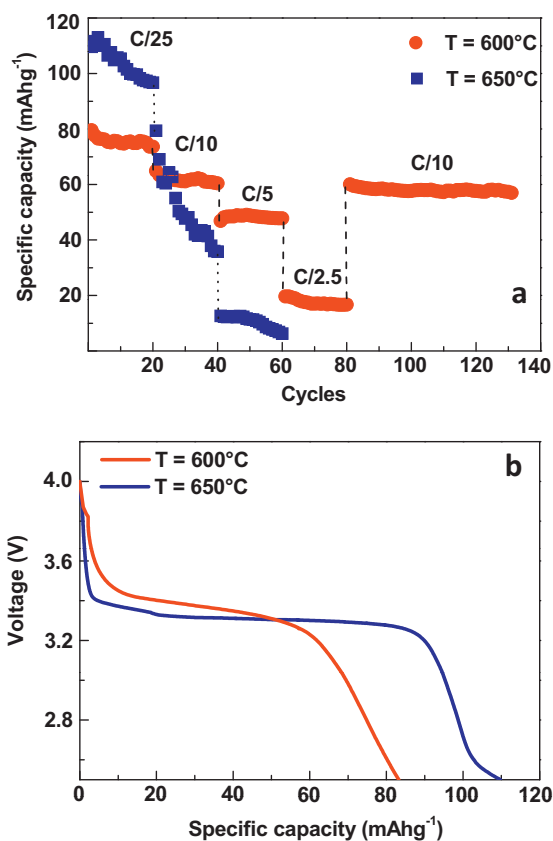


**Fig. 6.** (a) Discharge capacity, (b) discharge profile at C/25 discharge rate for carbon foam–LiFePO<sub>4</sub> composite samples that were annealed at increasing temperatures.

ical kinetics could be strongly inhibited and that high polarization overpotential is present. This overpotential emerges from a combination of Li-diffusion rates and the intrinsic activation barrier of transferring electrons which could be high due to the small size of the particles that is to say to the high interparticle surface.

Each of the samples was prepared into electrodes and cycled at least 20 times at different C-rates ranging from C/25 to C/2.5. The higher loading is 40–45 wt.% LiFePO<sub>4</sub> on carbon, a value which is in agreement with the data in [16]. The discharge capacities for the carbon foam/LiFePO<sub>4</sub> composites are presented in Fig. 6a. The annealing temperature had a significant effect on the capacity of the battery. The optimal temperature was determined to be  $600\text{ }^{\circ}\text{C}$  with a capacity of  $85\text{ mAh g}^{-1}$  attained at a discharge rate of C/25. Although the sample annealed at  $650\text{ }^{\circ}\text{C}$  delivered at the beginning a capacity of  $110\text{ mAh g}^{-1}$  at a rate of C/25, a capacity loss was observed during the cycling. This difference is even more evident at the slow discharge rate of C/10. This difference is likely due to the structural features of the composite materials. The discharge profiles in Fig. 6b have noticeably curved profiles even at such a low discharge rate of C/25. The 3.4 V voltage drops as the cell discharges due to polarization. This is due to the diffusion resistance within the composite electrode [21].

Although the materials presented in this paper did not achieve the values of the specific capacities widely reported in the literature; the novel concept offers promising structural enhancements. The concept implies a continuous porous carbon network which featured macro-, meso- and nanopores to act as a conductive and very lightweight current collector to which the LiFePO<sub>4</sub> can be infiltrated in order to improve access into the porous architecture and increase the interface between the carbon and the active electrode material.

#### 4. Conclusions

Composites of three-dimensional commercial foams coated with olivine structured lithium iron phosphates as cathode materials have been successfully prepared and investigated, to the best knowledge of the authors, for the first time. The composites have been prepared by soaking the foams in the starting solution, containing the ions. The olivine phase was identified by XRD analysis performed on powders, prepared under similar conditions. The surface investigation on the prepared composites after annealing at different temperatures (ranging between 600 °C and 700 °C) for 15 min showed a dependence of the morphology upon the used process as well as the annealing conditions. The composites showed a homogeneous coating of the olivine phase on the porous nanoarchitecture of the foams after soaking and annealing.

The electrochemical properties of the powders as well as of the composites were found to be dependent upon the annealing conditions. At the optimal annealing temperature (600 °C), the electrochemical measurements showed a good reproducibility of the peaks in the CV plots as well as narrower oxidation/reduction potential difference, which is representative of the good reversibility of the lithium extraction/insertion in the materials. The composites delivered a discharge capacity of 85 mAh g<sup>-1</sup> at a discharging rate of C/25 at room temperature for the sample annealed at 600 °C. Although the samples annealed at 650 °C delivered higher discharge capacity (110 mAh g<sup>-1</sup>, at a discharge rate of C/25 and room temperature), higher capacity loss was observed during the cycling.

In the future, improvements to the electrochemistry may be achieved by optimizing the coating of lithium iron phosphate surrounding the carbon foam. This would increase the carbon–LiFePO<sub>4</sub> interface and potentially improve the charge transfer kinetics. Further investigation into the application as e.g. supercapacitor electrode material may also be promising.

#### Role of funding source

The authors wish to thank the *Deutsche Forschungsgemeinschaft* (DFG) (Project: PAK-177) for the financial support during this work. The DFG promote and support financially the publication of the

scientific results obtained during the projects. The DFG had no involvement in study design; in the collection, analysis and interpretation of data; in the writing of the report, and in the decision to submit the paper for publication.

#### Acknowledgements

Many thanks are owed to Mr. J.-C. Jaud for the technical assistance in the XRD analysis. The Authors wish to thank gratefully the GRAFTECH France S.N.S. for supplying the carbon foams.

#### References

- [1] A.K. Padhi, K.S. Nanjundaswamy, J.B. Goodenough, *J. Electrochem. Soc.* 144 (1997) 1188.
- [2] D.H. Kim, J. Kim, *J. Phys. Chem. Solids* 68 (2007) 734.
- [3] A.S. Andersson, B. Kalska, L. Haggstrom, J.O. Thomas, *Solid State Ionics* 130 (2000) 41.
- [4] S.Y. Chung, J.T. Bloking, Y.M. Chiang, *Nat. Mater.* 2 (2002) 123.
- [5] A. Yamada, S.C. Chung, K. Hinokuma, *J. Electrochem. Soc.* 148 (2001) A224.
- [6] F. Croce, A. D'Epifanio, J. Hassoun, A. Deptula, T. Olazac, B. Scrosati, *Electrochem. Solid-State Lett.* 5 (2002) A47.
- [7] J. Barker, M.Y. Saidi, J.L. Swoyer, *Electrochem. Solid-State Lett.* 6 (3) (2003) A53.
- [8] R. Dominko, J.M. Goupil, M. Bele, M. Gaberscek, M. Remskar, D. Hanzel, J. Jamnik, *Electrochem. Solid-State Lett.* 152 (2005) A858.
- [9] J. Moskon, R. Dominko, M. Gaberscek, R. Cerc-Korošec, J. Jamnik, *J. Electrochem. Soc.* 153 (2006) A1805.
- [10] M.S. Bhuvaneshwari, N.N. Bramnik, D. Enslin, H. Ehrenberg, W. Jaegermann, *J. Power Sources* 180 (2008) 553.
- [11] J.W. Long, B. Dunn, D.R. Rolison, H.S. White, *Chem. Rev.* 104 (2004) 4463–4492.
- [12] C.M. Doherty, R.A. Caruso, B.M. Smarsly, P. Adelhelm, C.J. Drummond, *Chem. Mater.* 21 (2009) 5300–5306.
- [13] K.C. Kelley, C.F. Ostermeier, M.J. Maroon, Battery having carbon foam collector, Patent US20040121238 A1 (2004).
- [14] N. Brazis, K.C. Kelley, M.J. Maroon, B.I. Mohanov, Composite carbon foam, Patent WO2008020852 A1 (2008).
- [15] T.S. Moore, S. Dinda, Lithium ion battery utilizing carbon foam electrodes, Patent WO2000016418 A1 (2000).
- [16] N.J. Dudney, T.N. Tiegs, J.O. Kiggans, Y.-I. Jang, J.W. Klett, *ECS Transactions* 3 (27 Lithium-Ion Batteries), 2007, pp. 23–28.
- [17] L. Dimesso, C. Spanheimer, S. Jacke, W. Jaegermann, *Ionics* (2010), unpublished data.
- [18] M.P. Pechini, Method of preparing lead and alkaline earth titanates and niobates and coating method using the same to form a capacitor, Patent US3330697A (1967).
- [19] A.V. Murugan, S.C. Navale, V. Ravi, *Mater. Lett.* 60 (2006) 1023.
- [20] <http://www.graftec.com/PRODUCTS/Carbon-Foams.aspx>.
- [21] D. Choi, P.N. Kumta, *J. Power Sources* 163 (2007) 1064–1069.